Open Access

Recent Progress in Materials

LIDSEN Publishing Inc.

Original Research

Mechanical Characterization of a Tunable 3-D Collagen-Hyaluronic Acid Hydrogel for Use in Cell Culture

Jared Tucker [1], Victor Lai [2,*]

1. Department of Applied Materials Science, University of Minnesota-Duluth, 1303 Ordean Court, Duluth, United States of America; E-Mail: tucke449@d.umn.edu
2. Department of Chemical Engineering, University of Minnesota-Duluth, 1303 Ordean Court, Duluth, United States of America; E-Mail: laix0066@d.umn.edu

* **Correspondence:** Victor Lai; E-Mail: laix0066@d.umn.edu

Academic Editor: Khandaker M. Anwar Hossain

Special Issue: Development and Applications of Engineering Polymers

Recent Progress in Materials
2024, volume 6, issue 4
doi:10.21926/rpm.2404028

Received: June 28, 2024
Accepted: November 24, 2024
Published: December 17, 2024

Abstract

Many cells demonstrate variances in behavior due to their cell culture environment. To provide a mechanically-tunable, tissue-like environment, a 3D hydrogel for cell culture was formulated using collagen (Col) and hyaluronic acid (HA) to help provide a system for studying these dynamic cellular responses in a soft-tissue environment. A design of experiments was organized to study the effects of collagen concentration, HA fragment size, and Col: HA mass ratio on the hydrogel mechanical properties. Mechanical characterization of the gels was conducted using rheology and found that collagen concentration, but not HA content, directly modulated the hydrogel storage and loss modulus. The pore size of the hydrogels was also evaluated and found to trend directly with collagen concentration.

Keywords

Hydrogel; rheology; storage modulus; loss modulus; collagen; hyaluronic acid

1. Introduction

By definition, *in vitro* cellular studies aim to provide external, observable, and controlled conditions to better understand a function or behavior within an internal body. However, *in vitro* studies cannot provide a full understanding of cellular behavior due to the complexity of the *in vivo* conditions in which they are native. *In vitro* studies allow for a better understanding of biological systems such as the minutiae of gene regulation, cell secretions, and toxicology [1]. However, if the experimental conditions are not similar to the *in vivo* environment, false conclusions could be drawn. Thus, 3D cell culture provides a methodology for better understanding cellular behavior that normally occurs within a tissue environment. Part of the benefit of 3D cell culture is helping bridge the gap between traditional 2D *in vitro* studies and animal models [2]. Typically, for major studies, both *in vitro* and *in vivo* studies should be conducted alongside each other to verify whether the drawn conclusions are valid. Utilizing a well-designed 3D cell culture can help bolster confidence in cell culture studies and limit the necessity of additional *in vivo* animal studies.

1.1 Cell Culture in 2D vs 3D

In 2D cell culture, cell lines are traditionally grown on stiff substrates such as glass or polystyrene. These materials are typically characterized to have stiffnesses in the realm of GPa [3]. In comparison, tissue environments in the body can range from a few hundred Pa in soft tissues, such as hyaluronic acid (HA) and collagen, to a few hundred MPa for bone [4]. The *in vivo* conditions that many cell types grow in are dominated by tissues with moduli much lower than those of typical 2-D substrates [5]. Determining the mechanical conditions that cells grow in is imperative [6]. It has been shown in previous studies that many cells are influenced by their mechanical environment which may alter their chemical and biological behavior [7-9]. Thus, in this study, a soft-tissue-like hydrogel containing collagen and HA was formulated to provide a substrate for robust 3D cell culture and cellular behavior studies. This soft-tissue hydrogel was designed to mimic the mechanical and chemical environments within the extracellular matrix, in which cells are proliferated. However, the mechanical properties of the hydrogel must be understood prior to use as a cell culture substrate.

1.2 Hydrogel Mechanics

Since the stiffness of the extracellular matrix (ECM) is an important factor in cell culture, evaluating the structural properties of the hydrogel is critical. Biological hydrogels tend to be heterogenous, comprising of a scaffold of proteins and other biopolymers suspended in fluid [10]. These proteins such as collagen, hyaluronic acid, laminins, and proteoglycans are hydrophilic and often contain binding sites and signaling supports for the various cells in the matrix [11]. Mechanically, hydrogels are interesting materials to evaluate, as they are a dynamic mix of solid and liquid. While the polymer network acts as a backbone for the system, the fluid that is dispersed within the network is vital for providing additional support and energy dissipation. Some of the properties of interest for hydrogels are storage modulus, loss modulus, swelling, degradation, and mesh size [3]. Many hydrogels, especially with high fluid content and physical crosslinks, have high energy dissipation due to their relative softness and ability to deform [12]. One feature of hydrogels that is key for cell culture is the ability to modulate and evaluate pore size. In natural ECM environments, typically the pore size of the network is below the average cell diameter of 10

microns and is defined as nanoporous [13]. In such cases, the cells residing in the matrix must either rely on movement to deform enough to pass through the pores, such as with lamellipodial and lobopodial migration, or they can also secrete proteases to break down the matrix network [14]. For many hydrogels, the conditions which the gel is fabricated can influence the resulting porosity and pore size. Thus, it is important to consider the influences within the gelation environment and to identify the final porosity of the gels.

Another major property important to hydrogel characterization is the loss modulus and storage modulus. Hydrogels are generally classified as viscoelastic materials. As the term indicates, these materials possess properties that have both elastic (solid-like) and viscous (liquid-like) characteristics. Viscoelastic materials demonstrate a time-dependent behavior for many mechanical tests, similar to plastics [15]. Rheological testing can be utilized to evaluate these properties. The hydrogels respond uniquely to applied torque and the resulting strain can be evaluated to provide an understanding of the internal mechanics. Hydrogels are generally characterized as non-Newtonian where their viscosity is dependent on the shear rate [16].

1.3 Natural Hydrogels and Copolymers

Within the last few decades, the understanding and applications for natural polymers have steadily increased, showing an important opportunity for naturally-derived sources and sustainable polymer blends. Biopolymers such as chitin, cellulose, alginate, and starch have been at the forefront of readily available polymer sources whilst offering a variety of potential uses [17]. While some of the polymers within these groups have applications when used on their own, many of these materials gain much more usability once they are co-polymerized with another compound [18]. For example, strides have been taken to blend polyvinyl alcohol (PVOH) with starch, gelatin, chitosan, and cellulose to provide a biodegradable, naturally-sourced material in the food packaging industry [19]. Similar blends have also found applications in the medical technology, cosmetics, pharmaceuticals, and thin-films [20, 21].

1.4 Collagen and the Effect of HA in Hydrogel Cell Culture

For cell culture, natural protein-based polymers allow for mimicking the conditions within the ECM while providing a repeatable process for fabrication. Thus, to develop a robust and accurate cellular mechanical environment, collagen and HA were selected as key materials for this project. Collagen is ubiquitous in hydrogel cell culture and is easily sourced [22]. Collagen polymerizes easily in a controlled environment and provides a stable structure for both the hydrogel and the cells. Additionally, HA is a common glycosaminoglycan in many tissues, however it does not form polymeric chains unless synthetically crosslinked, e.g., with thiol groups to form disulfide crosslinkers [23]. The presence of HA has been shown to modulate the cellular activity of immune cells by eliciting an increased non-inflammatory response [24].

For 3D cell culture environments, utilizing non-crosslinked HA within a collagen network has been investigated previously. This study found that low molecular weight HA contributed to a slight increase the mechanical modulus of the hydrogel [25]. Additionally, the low molecular weight (MW) HA was found to influence the fibrillogenesis of the collagen due to having higher chain mobility than the higher MW HA [26]. Changes in rheological properties for varying final concentrations of HA have also been investigated, where the presence of HA in collagen slightly increased the storage

modulus of the gel; however, this was independent of the concentration of HA [27]. Interestingly, another study found the presence of high MW HA in collagen hydrogels decreased the aging mechanics of the gel, showing a greater decline in compressive modulus as compared to pure collagen hydrogels [28]. With respect to cell culture, HA has also been found to vary the behavior of certain immune cells depending on the MW of the HA present [24] However, the study did not investigate potential mechanical changes in the hydrogel based on HA fragment size of final concentration. Since cellular behavior is also modulated by the mechanical properties of the ECM, the correlation between cellular behavior and HA molecular weight may have been impeded by a limited scope of study.

Taken together, the goal of this work is to investigate how the fragment size and mass ratio of HA within a collagen hydrogel affect the mechanical structure and properties of the gel for potential use in cell culture studies. An experimental setup to investigate the effect of HA (fragment size and mass ratio) on the hydrogel's mechanical behavior will help us better understand the confounding mechanical and biomechanical effects of HA addition for future cellular behavior studies, providing a stronger basis to interpret those results.

2. Materials and Methods

2.1 Collagen-HA Hydrogel Fabrication

Sterile 15 mL centrifuge tubes (Thermo Fisher Scientific, Waltham, MA) were set aside for each gel composition being formulated and labeled correspondingly. Table 1 details the three levels of collagen concentration tested (0.75 mg/mL, 1.5 mg/mL, and 2.25 mg/mL) as well as the mass ratios of collagen to hyaluronic acid (0, 0.5, 1, and 2). Additionally, the fragment size of the HA was varied at the corresponding levels: 20 kDa, 500 kDa, and 2,000 kDa, resulting in a total of 36 combinations for this experimental design. For the experimental runs, five replicates of each combination of factors and levels were formulated and tested.

Table 1 The 3 factors and the corresponding levels of each used for the formulation of the collagen-HA co-gels. The experimental setup was executed using this combination of factors and levels. The mass ratio factor had 4 levels to allow for a pure collagen control for comparison.

Collagen Concentration (mg/ml)	HA Fragment Size (kDa)	Col: HA Mass Ratio
0.75	20	0
1.5	500	0.5
2.25	2,000	1
		2

To fabricate the gels, a similar procedure to previous work by Lai et al. was employed [29, 30]. 10× PBS buffer (Corning Life Sciences, Corning, NY) was added to each sterile 15 mL centrifuge tube. The volume of the 10× PBS varied depending on the formulation to keep the final hydrogel volume constant. Additionally, 150 mL of non-phenol red RPMI cell culture media (Corning Life Sciences, Corning, NY) was added to the tubes. At this point, the predetermined amount of sodium hyaluronate (NaHy) (Lifecore Biomedical, Chaska, MN) for each composition was weighed and

added. To ensure adequate dissolution into the buffer and media, the tubes were stirred for at least 30 seconds on a fixed-speed vortex mixer. The solution was then chilled to prevent gelation variabilities due to temperature differences. Next, refrigerated PureCol type-1 acid-solubilized bovine collagen (Advanced Biomatrix, Carlsbad, CA) was added to each vial with the appropriate volume for each composition. Lastly, 0.1 M sterile NaOH (Advanced Biomatrix, Carlsbad, CA) was added to each vial to neutralize the acidic solution and bring the pH between 7.2 and 7.4. The solutions were pipetted into 5 replicates within a 12-well plate system. The plate was placed into an incubator at 37°C and allowed to gel overnight.

2.2 Hydrogel Rheology

Rheology tests were performed on the gels using the Anton-Paar MCR 72 (Anton-Paar, Graz, AT) rheometer using a 25 mm diameter stainless steel parallel plate system. To prevent slippage during testing, 150 grit sandpaper was die cut and adhered to both parallel plate surfaces. A hydrogel sample was loaded onto the bottom, ensuring it extended the full diameter of the surface and the gap width was set at 5 mm. Of note, the compressive force and temperature could not be controlled using this rheometer model. Thus, the force was maintained using a constant height of 5 mm. Since this rheometer system was not equipped with a Peltier temperature control, the temperature of the samples was maintained and monitored via the temperature of the room which was kept at 22°C ± 2°C. The hydrogels were consistent in shape and morphology, being cast in the same well plates. Thus, gap distance control also provided consistent compressive force control across all samples. An amplitude sweep was conducted from 0.01% to 100% strain at a frequency of 10 rad/s, which was used as the upper limit of frequency [6, 11]. The LVER was then determined at the inflection point of the decline in G', which was an indication of the material having permanent deformations within the polymer matrix.

Subsequently, the maximum strain before the end of the LVER was used for further analysis using a frequency sweep, varying from 1 rad/s to 10 rad/s, following previous published methodologies [6]. The resulting plot was averaged across the entire data range to find the corresponding G' and G'' for the gels. Statistical significance was found using Tukey's test. Equation 1 provides the formula for finding the Honestly Significant Difference, the difference required for statistical significance. In the equation, σ denotes the mean standard deviation for each sample set, and N denotes the sample size of each group.

$$HSD = \frac{Mean_1 + Mean_2}{\sqrt{\frac{1}{2} * \left(\frac{\sigma_1 + \sigma_2}{2}\right) * \left(\frac{1}{N_1} + \frac{1}{N_2}\right)}} \quad (1)$$

2.3 Collagen Staining and Imaging

For imaging, 5- (and-6)-Carboxytetramethylrhodamine Succinimidyl Ester (TAMRA-SE) (Thermo Fisher Scientific, Waltham, MA) was used to fluorescently stain the collagen fibrils within the hydrogel according to the procedure outlines by Sapudom et al. [31]. A 3% TAMRA-SE solution was prepared with dimethylformamide (DMF) (Millispore Sigma, Burlington, MA) and then aliquoted into 1.5 mL batches. To evaluate gel porosity based on collagen concentration and HA content, hydrogel samples were formulated at 0.75 mg/mL, 1.5 mg/mL, and 2.25 mg/mL collagen

concentration following the previously described procedure. Additionally, to evaluate any effect due to HA, medium collagen concentration gels were fabricated with 20 kDA, 500 kDa, and 2,000 kDa HA fragment size. 10 µL of TAMRA-SE solution was added to each gel sample after gelation. The sample was then placed in an incubator at 37°C for one hour. The gels were then rinsed with 10× PBS at least 5 times by adding 300 mL of PBS to the top of each hydrogel diffusing for 15 minutes. The solution was pipetted off of the hydrogel and the process was repeated until the red TAMRA-SE was no longer visible.

Once fluorescently labeled, a Nikon Ti2 laser confocal microscope (Nikon, Tokyo, JP) was used to image the gels. All images were collected using laser confocal at a wavelength of 550 nm to excite Red Fluorescent Protein (RFP), used Galvano scanning with averaging of 16 at a maximum field of view, and a z-stack step size of 25 microns. Confocal images were collected at the bulk of the matrix to find the average pore size. Pore size analysis was conducted in Fiji and statistical significance was evaluated using a Tukey's T-test in Excel.

2.4 Pore Size Determination

In order to quantify the pore size of the matrix, three replicate samples of each collagen composition were imaged using fluorescent microscopy and analyzed in Fiji using a method similar to other published works [32, 33]. The recorded images were first processed using thresholding. This process binarizes the image based on a lower limit of pixel intensity to distinguish fibrils that are on the same layer height. Thus, by limiting the matrix to higher intensities, a monolayer of fibrils within the same focal plane can be generated. After thresholding, five pores were chosen at random and measured using an oval drawing tool in Fiji (Figure 1). The oval was drawn to match the pore as best as possible, and the five areas were measured and the average for each composition was found. Statistical significance testing was run in Excel to investigate any differences in pore size due to collagen concentration.

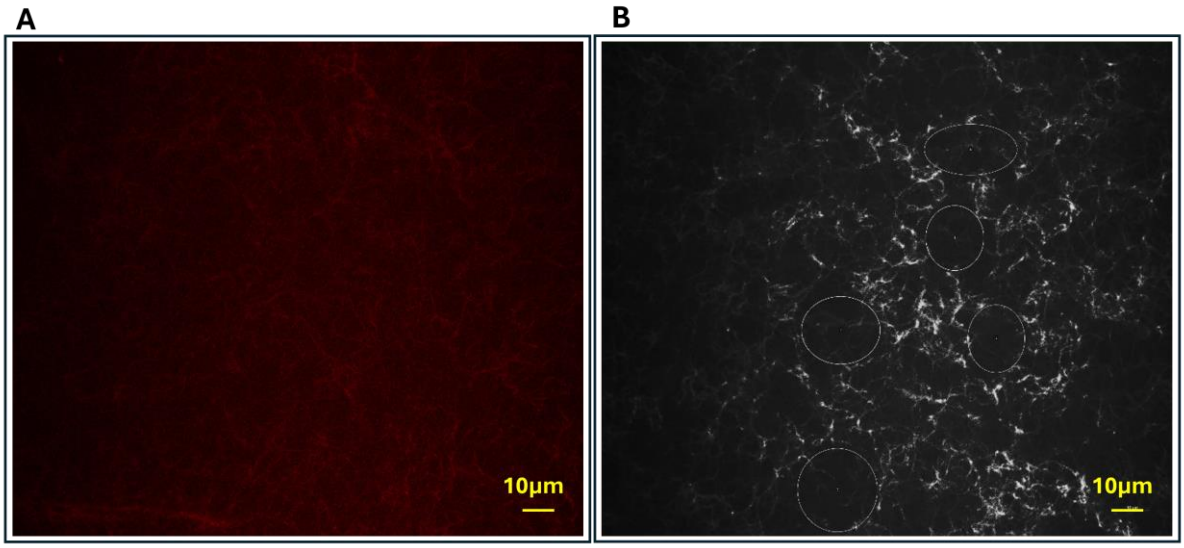

Figure 1 A) The raw image of a 0.75 mg/mL collagen sample with 20 kDa HA under 40× magnification prior to thresholding. B) The same image after thresholding with the pore area measurements being modeled by ovals in Fiji. The areas were collected on each replicate for each concentration and were averaged to find the mean pore size.

3. Results

3.1 LVER Determination

The first set of experiments identified the LVER for these hydrogels. Using a second derivative evaluation, as shown in the example amplitude sweep for a Col-HA gel in Figure 2, the sharpest decrease in G' began just before 1% strain. Thus, the maximum strain rate before permanent deformation was estimated to be just below 1%, which is consistent with other studies [16, 27, 34]. However, due to the limitations of the mechanical bearing rheometer for high precision, low-strain testing, 1% strain was chosen to balance higher resolution data with being as close to the LVER as possible.

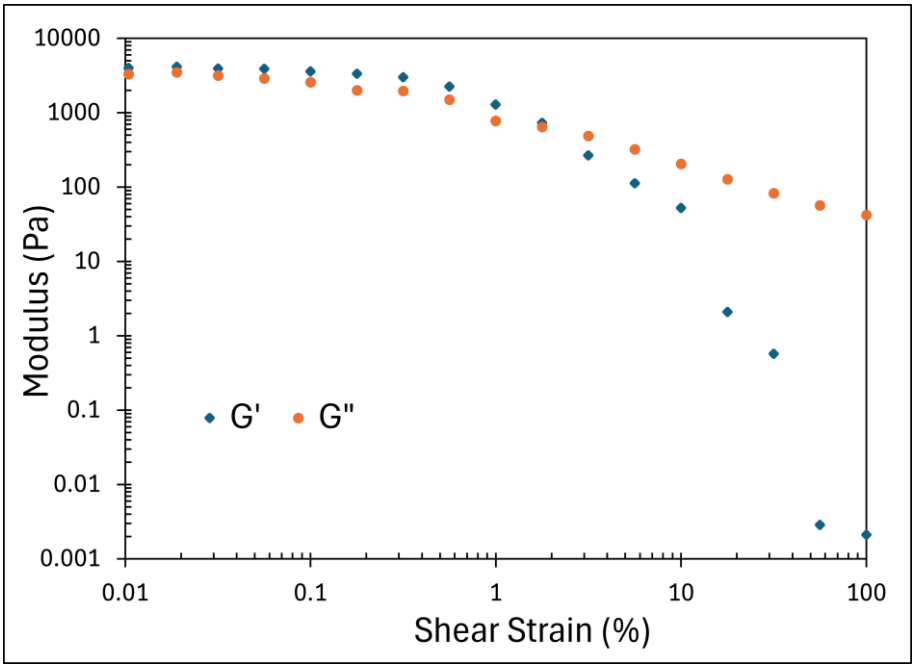

Figure 2 An example amplitude sweep for the Col-HA co-gel system with a composition of 2.25 mg/mL, 20 KDa HA, and 1:1 mass ratio. While the storage modulus decreased slightly in the low strain ranges, an inflection point was identified at a frequency of approximately 1 rad/s, indicating a sharp decrease in storage modulus.

This strain amplitude of 1% was used for the next phase of rheologic analysis. 10 data points were obtained by varying the angular frequency from 1 rad/s to 10 rad/s (example shown in Figure 3), and these values were averaged to obtain the G' and G" of each sample. The results were then categorized based on the sample's composition and the main effects plots were generated.

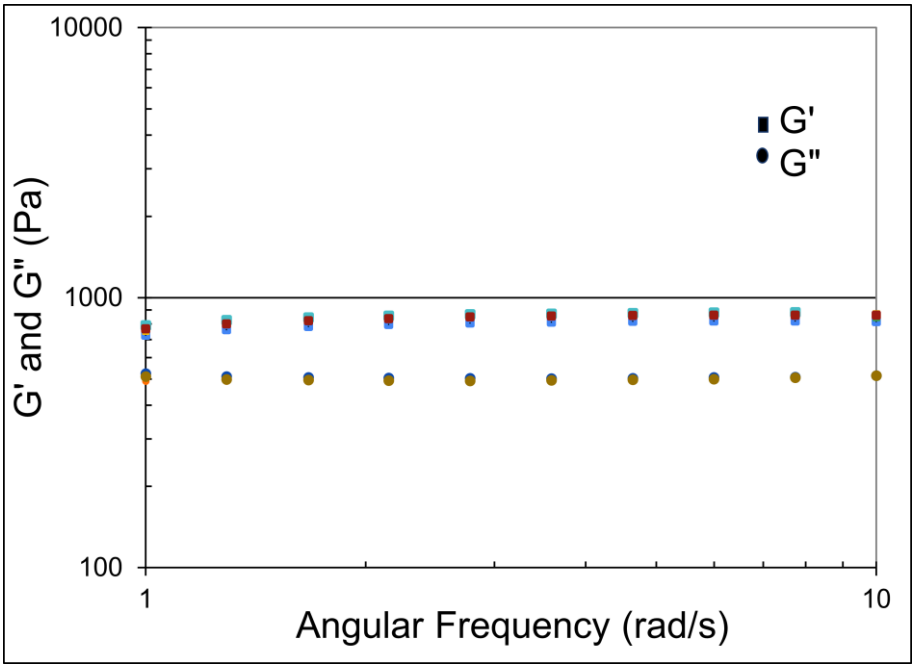

Figure 3 Characteristic data for G' and G'' of a 1.5 mg/mL, 500 kDa, 1:1 mass ratio sample in the screening experimental run. The G' was greater than the G'', indicating a structural solid. A mean value of G' and G'' for each run was obtained by averaging all values across the range of frequencies.

3.2 Effect of Col Concentration, Col-HA Mass Ratio, and HA Fragment Size

For each of the compositions, the five replicate samples were tested using the previously described frequency sweep parameters. The resulting data was averaged across the 1 rad/s to 10 rad/s range to find a singular G' and G" value for each sampling. The main effects plots for each grouping were then generated in Excel and analyzed using Tukey's modified t-test to evaluate statistical significance. The results were compiled as shown in Figure 4.

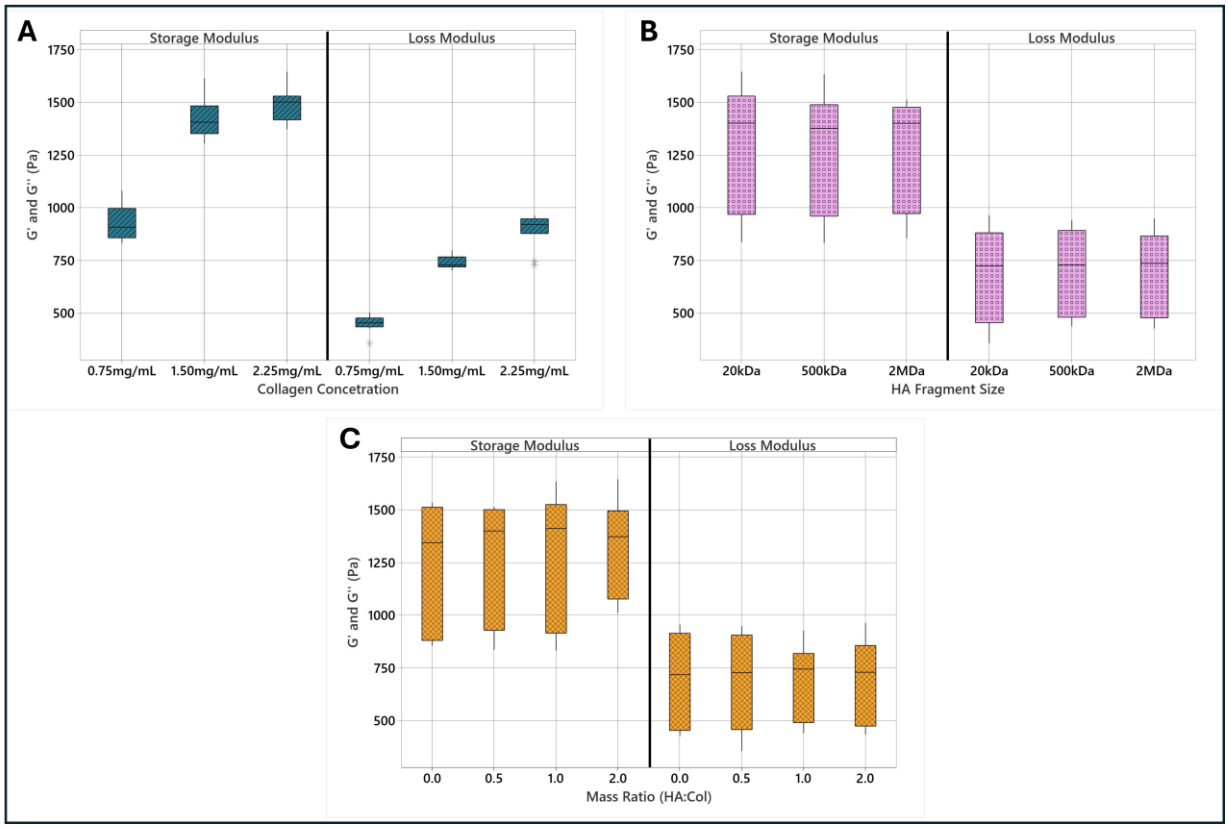

Figure 4 The main effects plots for the hydrogel rheology experiments. (A) Collagen concentration: There was a statistically significant increase in G' and G'' with increasing collagen concentration. (B) HA fragment size: No significant trend was observed in G' and G'' with varying HA fragment size. (C) Col: HA mass ratio: No significant trend was observed in G' and G'' with varying mass ratios. (* indicates a p-value < 0.05, n = 60 for each grouping).

The main effects plots show a distinct trend in G' and G'' with collagen concentration (Figure 5A). A statistically significant difference was observed between the 0.75 mg/mL and 2.25 mg/mL samples. A non-linear relationship was observed as there was a more distinct increase in G' between the 0.75 mg/mL and 1.5 mg/mL samples when compared to the 1.5 mg/mL and 2.25 mg/mL increase. No statistical differences in G' and G" were observed with changes in HA fragment size (Figure 4B) or HA: Col mass ratio (Figure 4C). The final concentration of HA within the co-gels ranged between 0.375 mg/mL and 4.5 mg/mL based on the selected mass ratio and collagen concentration in each sample. These HA concentrations are physiologically relevant as they fall well within the ranges found within human tissue [23]. However, no trend was found in G' or G" with the increase in HA concentration.

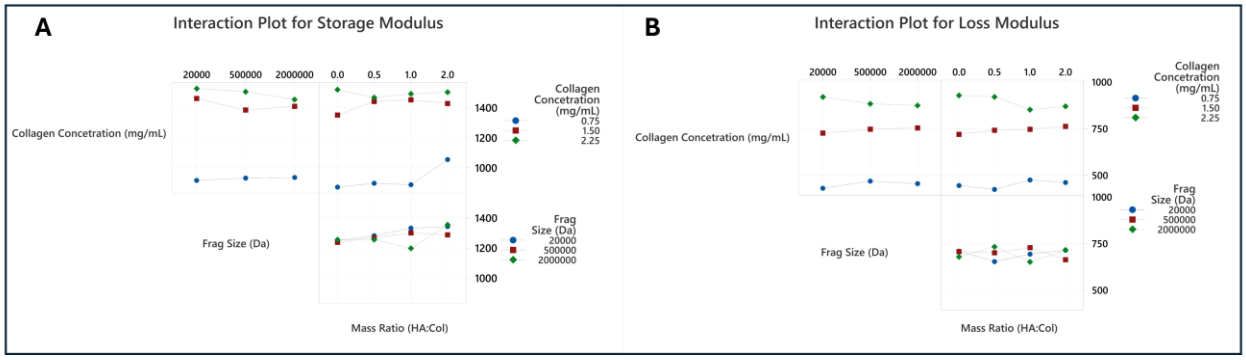

Figure 5 A) The interaction plots between collagen concentration, HA fragment size, and mass ratio for G'. No statistically significant linear trends were observed for the interactions of the factors. B) The interaction plots between collagen concentration, HA fragment size, and mass ratio for G". No statistically significant linear trends were observed for the interactions of the factors. Of note, the significant change in G' and G" in the top row of the graph are influenced solely by the changes in collagen concentration.

The interaction plots between the experimental factors were generated using Minitab and did not yield any significant trends. Given that collagen concentration was found to be the driving force behind the changes in G' and G" from the main effects plots, it is unsurprising that no significant impact was found between collagen and HA. While a slight increase in G' based on the interaction between HA fragment size and mass ratio was observed, this difference was not statistically significant. Broadening the range of these two factors could illustrate a fuller picture of the interaction.

3.3 Collagen Gel Porosity

Figure 6 shows the results of pore size with collagen concentration. The resulting pore sizes showed a distinct trend with collagen concentration. At low collagen concentrations, the pore sizes were large and decreased as concentration increased. The average pore size was found to be statistically significant between all pairs of collagen concentration samples. A larger decrease in pore size was observed when collagen concentration increased from 0.75 mg/mL to 1.5 mg/mL, compared 1.5 mg/mL to 2.25 mg/mL. Interestingly, this qualitative observation is similar to the magnitude of change in G' and G" with increasing collagen concentration as seen in Figure 3A.

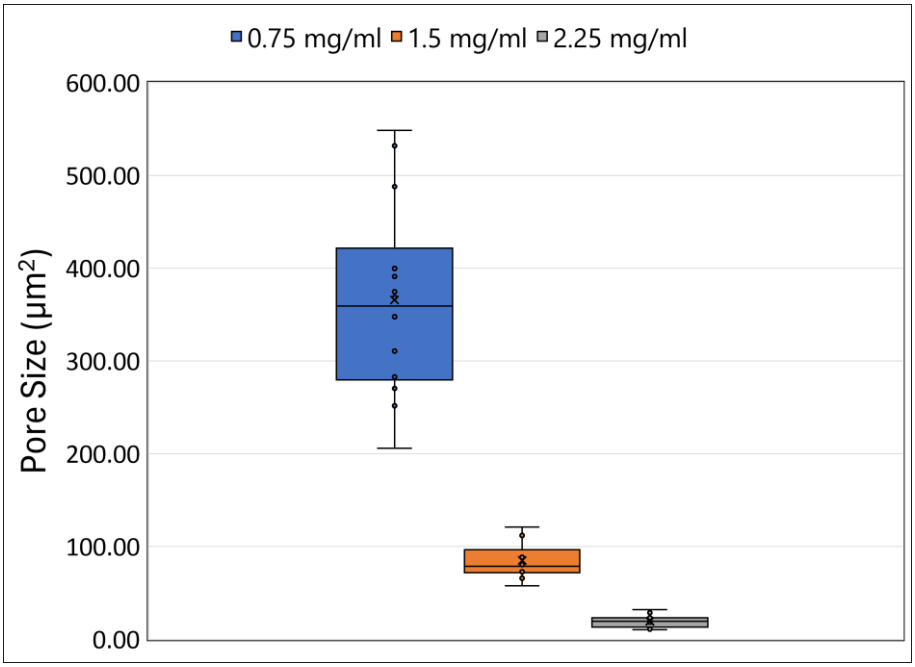

Figure 6 The pore size distribution for each collagen concentration. Each grouping had a sample size of 15 and was recorded from 3 separate images. A statistically significant difference was found between each concentration (* indicates a p-value < 0.05).

4. Discussion

Our rheology results showing an increase in G' with collagen concentration are consistent with other published research on the viscoelastic properties of collagen gels [16]. Since collagen is the main structural component in these hydrogels, higher concentrations of collagen would result in a greater number of collagen fibrils in the network gels, in turn increasing the G'. This observation has been observed in previous research studies [35-37], and this was also evident in this work as well. Interestingly, the G" also showed an increase with greater collagen concentration. That viscoelastic properties vary with polymer molecular weights and chain lengths are well-documented [33, 38-40], however, little work has been conducted to correlate polymer concentration and G". We hypothesize that the starting concentration of collagen solution alters the way the collagen polymerizes, hence changing the average molecular weight of the resulting hydrogels which affects its viscoelastic properties. Thus, the collagen solution that is left in the interstitial space of the hydrogel would increase the viscosity of the solution, increasing the G". Testing this hypothesis will require further experimental characterization on the microstructure and properties of the polymerized collagen network.

Importantly, there was no observed effect on G' or G" due to HA fragment size or mass ratio. Since the HA does not polymerize or form a gel of its own, the HA molecules are presumed to remain within the solution, in the interstitial space of the collagen network. Our results suggest that, while the HA molecules can still interact with the collagen network, they do not add to the overall mechanical structure of the network. The lack of statistical difference in loss modulus with HA mass ratio suggests that, similar to the storage modulus, the viscous behavior of these Col-HA hydrogels is also dominated by the collagen network and the unpolymerized collagen remaining in solution.

Taken together, these results are especially important in interpreting changes in cellular behavior in Col-HA gels in studies such as those by Rayahin et al. [24]. Previous studies have changes in cellular behavior due to the presence of HA within the hydrogels, showing a modulated cell behavior to either pro-inflammatory or anti-inflammatory based on the HA molecular weight. However, these studies have wholistically neglected to investigate any mechanical changes within the hydrogel due to changes in HA additions. Thus, this work would indicate that there are no significant mechanical changes due to varying HA fragment size or concentration within the ranges tested in this work, indicating that the results observed in these previous studies are not confounded by mechanical changes in the system.

Since the storage modulus and loss modulus of the hydrogel are directly linked to the collagen concentration, it is expected that the pore size would also be affected. With a greater collagen density, the number of fibrils present increases within the system and the amount of void space within the network decreases, hence decreasing the pore size. Thus, this result of larger pore size at low-concentration collagen and smaller pore size in high-concentration collagen matches with the previous result of increasing G' and G" with increased collagen density [35, 36]. Few research investigating the effects of loss modulus on the porosity of hydrogels has been performed to date to corroborate our observed result of decreased porosity with increased loss modulus. We postulate that since the concentration of collagen within the pre-gelled solution affects the final fibril size and network density, the energy required to disperse fluid is increased due to a decrease in void volume. This decrease in interstitial space for the fluid, in tandem with a more densely structured collagen network, resists the dispersal of energy through fluid flow to increase G" accordingly.

The pore size analysis that was conducted assumed that collagen provided the core physical structure of the hydrogel, as HA was not physically crosslinked. This assumption resulted in staining solely the collagen for fluorescent imaging. While this allowed for an understanding of how collagen concentration affected the pore structure, it limited the conclusions of how HA content affected pore size. The images collected were manually measured for pore size, as the images that were recorded displayed a variation in depth-of-field that did not allow for program-based pore calculations. The manual measurement followed a geometry estimation similar to previous works [32, 33]. Future work on this topic could focus on the direct pore size effects due to HA fragment size and concentration through additional staining of the HA. Imaging of these samples could continue to bolster that understanding of the structures present in the collagen-HA co-gel system.

Overall, results from this collagen staining experiment showed that the pore sizes of the collagen matrices were smaller than the average size of typical cells. At the largest pore size (in the low-concentration collagen), the voids had an average size of 360 μm^2. By assuming that the pores could be modeled as circular, it was found that the average diameter of the largest pores was 10.7 square micrometers. This is notable because it is less than half the average diameter of a cell such as a macrophage (~21 μm) [41, 42]. While this would not completely inhibit cell movement due to their ability to digest the matrix with proteases, it is likely to reduce cell movement in other modes. Additional studies could be organized to track cell gene expression or activation that may be linked with either motility mode to determine if the macrophages are exhibiting any biological indication of motility. It remains a tenuous connection that the size of the pores may be limiting the freedom of movement of the macrophages in the collagen-HA hydrogel.

5. Conclusions

Through the use of rheology, it was found that the G' and G" of the hydrogel increased directly with collagen concentration but were not affected by either HA mass ratio or fragment size. This implies that the gel mechanical properties will not be altered due to the addition or variation of HA content even though the biochemical composition would be altered. As the collagen concentration increased, the density of the network of collagen fibrils also increased, providing more stability for the structure. This, in turn, increased the storage modulus of the hydrogels and decreased the average pore size. Ultimately, this project was an intertwining of the mechanical aspects of the collagen-HA hydrogel with the future potential of microbiological characterization for cell culture studies. The evidence that the HA size and mass ratio had no effect on either G' or G'' was novel information and critical to understanding the cellular trends in the future. It also aids in the ability to tune the properties of the gel as desired.

Acknowledgments

We acknowledge Dr. Benjamin Clarke (Professor, Department of Biomedical Sciences, University of Minnesota) and Shannon Redbrook (Research Assistant, Department of Biomedical Sciences, University of Minnesota) for their help and advice with the research.

Author Contributions

Jared Tucker: ran all experiments, analyzed data, co-wrote manuscript. Victor Lai: Principal Investigator, generated ideas for the research, obtained funding, co-wrote manuscript.

Funding

This research was funded by the University of Minnesota Duluth Executive Vice Chancellor for Academic Affairs (EVCAA) Research and Scholarship Grant Program.

Competing Interests

The authors have declared that no competing interests exist.

References

1. Chen M, Zhang Y, Zhou P, Liu X, Zhao H, Zhou X, et al. Substrate stiffness modulates bone marrow-derived macrophage polarization through NF-κB signaling pathway. Bioact Mater. 2020; 5: 880-890.
2. Baker BM, Chen CS. Deconstructing the third dimension-how 3D culture microenvironments alter cellular cues. J Cell Sci. 2012; 125: 3015-3024.
3. Caliari SR, Burdick JA. A practical guide to hydrogels for cell culture. Nat Methods. 2016; 13: 405-414.
4. Hart NH, Nimphius S, Rantalainen T, Ireland A, Siafarikas A, Newton RU. Mechanical basis of bone strength: Influence of bone material, bone structure and muscle action. J Musculoskelet Neuronal Interact. 2017; 17: 114-139.

5. Koledova Z. 3D cell culture: An introduction. In: 3D cell culture: Methods in molecular biology. New York, NY: Humana Press; 2017. pp. 1-11.
6. Zhang Y, Wang Z, Sun Q, Li Q, Li S, Li X. Dynamic hydrogels with viscoelasticity and tunable stiffness for the regulation of cell behavior and fate. Materials. 2023; 16: 5161.
7. Martino F, Perestrelo AR, Vinarský V, Pagliari S, Forte G. Cellular mechanotransduction: From tension to function. Front Physiol. 2018; 9: 824.
8. Mennens SF, van den Dries K, Cambi A. Role for mechanotransduction in macrophage and dendritic cell immunobiology. In: Macrophages: Origin, functions and biointervention. Cham: Springer; 2017. pp. 209-242.
9. Chen Z, Wang L, Guo C, Qiu M, Cheng L, Chen K, et al. Vascularized polypeptide hydrogel modulates macrophage polarization for wound healing. Acta Biomater. 2023; 155: 218-234.
10. Chaudhuri O. Viscoelastic hydrogels for 3D cell culture. Biomater Sci. 2017; 5: 1480-1490.
11. Sun B. The mechanics of fibrillar collagen extracellular matrix. Cell Rep Phys Sci. 2021; 2: 100515.
12. Norioka C, Inamoto Y, Hajime C, Kawamura A, Miyata T. A universal method to easily design tough and stretchable hydrogels. NPG Asia Mater. 2021; 13: 34.
13. Tibbitt MW, Anseth KS. Hydrogels as extracellular matrix mimics for 3D cell culture. Biotechnol Bioeng. 2009; 103: 655-663.
14. Yamada KM, Collins JW, Cruz Walma DA, Doyle AD, Morales SG, Lu J, et al. Extracellular matrix dynamics in cell migration, invasion and tissue morphogenesis. Int J Exp Pathol. 2019; 100: 144-152.
15. Oyen ML. Mechanical characterisation of hydrogel materials. Int Mater Rev. 2014; 59: 44-59.
16. Gong J, Wang L, Wu J, Yuan Y, Mu RJ, Du Y, et al. The rheological and physicochemical properties of a novel thermosensitive hydrogel based on konjac glucomannan/gum tragacanth. LWT. 2019; 100: 271-277.
17. Silva AC, Silvestre AJ, Vilela C, Freire CS. Natural polymers-based materials: A contribution to a greener future. Molecules. 2021; 27: 94.
18. Yu L, Dean K, Li L. Polymer blends and composites from renewable resources. Prog Polym Sci. 2006; 31: 576-602.
19. Panda PK, Sadeghi K, Seo J. Recent advances in poly (vinyl alcohol)/natural polymer based films for food packaging applications: A review. Food Packag Shelf Life. 2022; 33: 100904.
20. Silva NH, Vilela C, Marrucho IM, Freire CS, Neto CP, Silvestre AJ. Protein-based materials: From sources to innovative sustainable materials for biomedical applications. J Mater Chem B. 2014; 2: 3715-3740.
21. Vilela C, Pinto RJ, Pinto S, Marques P, Silvestre A, Barros CS. Polysaccharide based hybrid materials: Metals and metal oxides, graphene and carbon nanotubes. Cham: Springer; 2018.
22. Chua P, Lim WK. The strategic uses of collagen in adherent cell cultures. Cell Biol Int. 2023; 47: 367-373.
23. Snetkov P, Zakharova K, Morozkina S, Olekhnovich R, Uspenskaya M. Hyaluronic acid: The influence of molecular weight on structural, physical, physico-chemical, and degradable properties of biopolymer. Polymers. 2020; 12: 1800.
24. Rayahin JE, Buhrman JS, Zhang Y, Koh TJ, Gemeinhart RA. High and low molecular weight hyaluronic acid differentially influence macrophage activation. ACS Biomater Sci Eng. 2015; 1: 481-493.

25. Xin X, Borzacchiello A, Netti PA, Ambrosio L, Nicolais L. Hyaluronic-acid-based semi-interpenetrating materials. J Biomater Sci Polym Ed. 2004; 15: 1223-1236.
26. Xu Q, Torres JE, Hakim M, Babiak PM, Pal P, Battistoni CM, et al. Collagen-and hyaluronic acid-based hydrogels and their biomedical applications. Mater Sci Eng R Rep. 2021; 146: 100641.
27. Yang YL, Kaufman LJ. Rheology and confocal reflectance microscopy as probes of mechanical properties and structure during collagen and collagen/hyaluronan self-assembly. Biophys J. 2009; 96: 1566-1585.
28. Chen S, Zhang Q, Kawazoe N, Chen G. Effect of high molecular weight hyaluronic acid on chondrocytes cultured in collagen/hyaluronic acid porous scaffolds. RSC Adv. 2015; 5: 94405-94410.
29. Lai VK, Nedrelow DS, Lake SP, Kim B, Weiss EM, Tranquillo RT, et al. Swelling of collagen-hyaluronic acid co-gels: An *in vitro* residual stress model. Ann Biomed Eng. 2016; 44: 2984-2993.
30. Vidmar CS, Bazzi M, Lai VK. Computational and experimental comparison on the effects of flow-induced compression on the permeability of collagen gels. J Mech Behav Biomed Mater. 2022; 128: 105107.
31. Sapudom J, Rubner S, Martin S, Kurth T, Riedel S, Mierke CT, et al. The phenotype of cancer cell invasion controlled by fibril diameter and pore size of 3D collagen networks. Biomaterials. 2015; 52: 367-375.
32. Kreger ST, Voytik-Harbin SL. Hyaluronan concentration within a 3D collagen matrix modulates matrix viscoelasticity, but not fibroblast response. Matrix Biol. 2009; 28: 336-346.
33. Arevalo RC, Urbach JS, Blair DL. Size-dependent rheology of type-I collagen networks. Biophys J. 2010; 99: PL65-L67.
34. Stojkov G, Niyazov Z, Picchioni F, Bose RK. Relationship between structure and rheology of hydrogels for various applications. Gels. 2021; 7: 255.
35. Fischer T, Hayn A, Mierke CT. Fast and reliable advanced two-step pore-size analysis of biomimetic 3D extracellular matrix scaffolds. Sci Rep. 2019; 9: 8352.
36. Hayn A, Fischer T, Mierke CT. Inhomogeneities in 3D collagen matrices impact matrix mechanics and cancer cell migration. Front Cell Dev Biol. 2020; 8: 593879.
37. Antoine EE, Vlachos PP, Rylander MN. Review of collagen I hydrogels for bioengineered tissue microenvironments: Characterization of mechanics, structure, and transport. Tissue Eng Part B Rev. 2014; 20: 683-696.
38. Cooper-White JJ, Mackay ME. Rheological properties of poly (lactides). Effect of molecular weight and temperature on the viscoelasticity of poly (l-lactic acid). J Polym Sci B Polym Phys. 1999; 37: 1803-1814.
39. Kurata M, Osaki K, Einaga Y, Sugie T. Effect of molecular weight distribution on viscoelastic properties of polymers. J Polym Sci Polym Phys Ed. 1974; 12: 849-869.
40. Cacopardo L, Guazzelli N, Nossa R, Mattei G, Ahluwalia A. Engineering hydrogel viscoelasticity. J Mech Behav Biomed Mater. 2019; 89: 162-167.
41. Lendeckel U, Venz S, Wolke C. Macrophages: Shapes and functions. ChemTexts. 2022; 8: 12.
42. Krombach F, Münzing S, Allmeling AM, Gerlach JT, Behr J, Dörger M. Cell size of alveolar macrophages: An interspecies comparison. Environ Health Perspect. 1997; 105: 1261-1263.